Groove-Buried Optical Waveguides Based on Metal Organic Solution-Derived $Ba_{0.7}Sr_{0.3}TiO_3$ Thin Films

Zhimou Xu, Masato Suzuki, Yuichiro Tanushi, Keita Wakushima and Shin Yokoyama
Research Center for Nanodevices and Systems, Hiroshima University,
1-4-2 Kagamiyama, Higashi-Hiroshima 739-8527, Japan
Phone: +81-82-424-6265, Fax: +81-82-424-3499, Email: yokoyama@sxsys.hiroshima-u.ac.jp

1. Introduction

Recently, much attention has been paid to $(Ba_xSr_{1-x})TiO_3$ (BST) thin films in integrated opto-electronic device applications as they have prominent properties such as large electro-optic coefficient and low optical losses. In this work, a groove-buried type optical waveguide and a Mach-Zehnder switching based on metal organic solution-derived $Ba_{0.7}Sr_{0.3}TiO_3$ (BST0.7) thin film core layer were introduced.

2. Experiments

A groove-buried optical waveguide was constructed with BST0.7-based core layer and SiO_2 cladding layer. The layout cross section of the BST0.7-based optical waveguide is shown schematically in Fig.1. Figure 2 shows the fabrication process flow. The BST0.7 thin films were fabricated by metal organic decomposition (MOD) technique. The Mach-Zehnder switching with poly-BST0.7 core layer was fabricated by traditional micro-fabrication methods.

3. Results and discussion

Figure 3 shows XRD patterns of about 200 nm thick BST0.7 films postannealed at different temperature. The substrate was fused quartz. A complete pseudo-cubic perovskite phase of BST0.7 appeared at 550℃ for 2h-postannealing. The as-deposited films were amorphous.

Figure 4 depicts the optical transmittance spectra of BST0.7 thin films on fused quartz. All the BST0.7 thin films were highly transparent to light for wavelengths longer than about 370 nm.

In general, high density photonic devices require the use of sharp, e.g. 90°, bends. The BST 90° bend waveguide structure shown in Fig. 5 was designed on the basis of a double corner mirror structure [1]. The waveguide bend transition angle θ=22.7° was adopted in this work. The relation between the bent transition distance l and the width w of the waveguide is given by $l = 3.4w$. The bend size was small, $34\mu m \times 34\mu m$, for an optical waveguide with the width of 10 μm (SEM picture shown in Fig. 5).

To perform the cutback measurement, the different length waveguides including one bend and three bends (as shown in Fig. 6) were prepared and the transmission of $\lambda = 632.8nm$ light through the waveguide was measured. Assuming the intensity of output light from the waveguide including one bend and three bends are I_{out1} and I_{out2} respectively, their relation can be given as

$$\ln I_{ratio} = 2\ln T - \alpha \bullet \Delta L \qquad (1)$$

where $I_{ratio} = \frac{I_{out2}}{I_{out1}}$, $\Delta L = L'_{total} - L_{total}$. L'_{total} and L_{total} are respectively equal to the total length of a waveguide including three bends and one bend, for example $L'_{total} = L'_1 + L'_2 + L'_3 + L'_4$. α is the absorption coefficient of waveguide. T is the optical transmission of the 90° bend. The optical propagation loss α_L and 90° bend loss α_b can be calculated from extrapolation of the plot of $\ln I_{ratio}$ versus ΔL. Figure 7 and Figure 8 show the optical losses of amorphous and polycrystalline (postannealed at 550°C for 2h) BST0.7 thin film groove-buried waveguides with the width of 5 μm respectively. It was found that the optical propagation losses were about 12.8 and 17 dB/cm respectively for amorphous and polycrystalline thin films. The 90° bend loss was about 1.2 dB for 5 μm wide amorphous BST0.7 waveguides. Comparing sputtering with MOD method, it can be seen that the polycrystalline BST films fabricated by MOD had lower optical propagation losses (as shown in Fig. 9). In addition, the bend loss of the 90° bent waveguide with a small curvature of micrometers was small which was helpful to make photonic device size scale down and realize the high density integration.

Figure 10 shows the output light intensity versus time for a Mach-Zehnder switching with 5 μm wide and 350 nm thick poly-BST0.7 core layer when applied bias voltage (a) and no bias (b) respectively. The light phase shift has been realized when applied low bias voltage. This illustrates that poly-BST0.7 thin films having electro-optic effects have been fabricated by MOD method successfully.

4. Conclusions

In summary, the $Ba_{0.7}Sr_{0.3}TiO_3$ (BST0.7) thin film groove-buried waveguides with 90° bent structure have been successfully fabricated on Si substrates with 1.65 μm thick SiO_2 thermal oxide layer by using a metal organic decomposition (MOD)-spin-coating procedure. The optical propagation losses were about 12.8 and 17dB/cm respectively for amorphous and polycrystalline thin films. The poly-BST0.7 thin films also have electro-optic effects. The light phase shift of a Mach-Zehnder switching with poly-BST0.7 core layer has been realized when applied low bias voltage.

Acknowledgements

This study was supported in part by 21st Century COE program "Nanoelectronics for Tera-Bit Information Processing" from the Ministry of Education, Culture, Sports, Science and Technology, Japanese Government.

References

[1] R. L. Espinola, R. U. Ahmad, F. Pizzuto, M. J. Steel and R. M. Osgood, Jr. , Optics Express, 8, (2001).

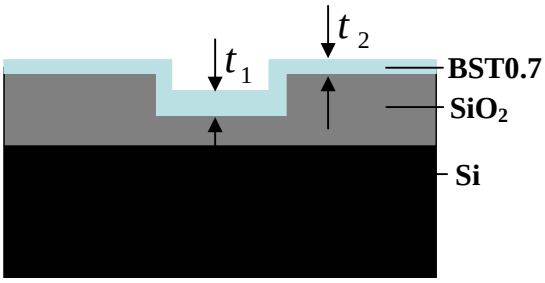

Fig. 1. The layout cross section of the amorphous BST0.7 thin film groove-buried optical waveguide.

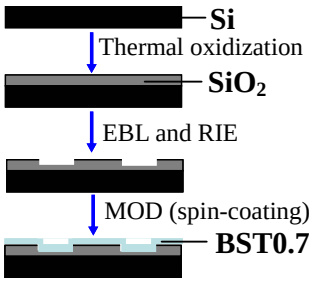

Fig. 2. Fabrication process flow for the amorphous BST0.7 thin film groove-buried optical waveguide.

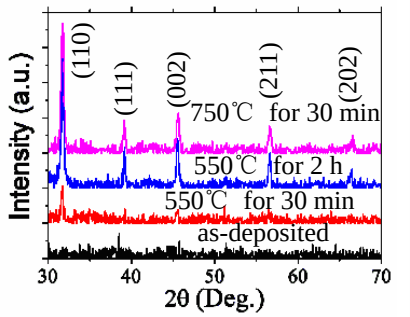

Fig. 3. XRD patterns of about 200 nm thick BST0.7 thin films on fused quartz substrates.

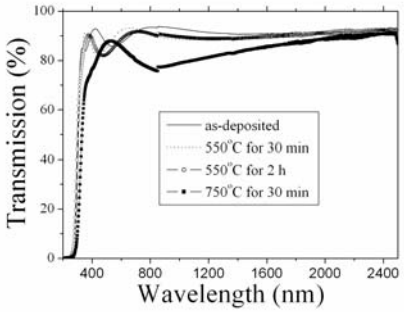

Fig.4. Transmittance spectra of about 200 nm thick BST0.7 thin films on fused quartz substrates.

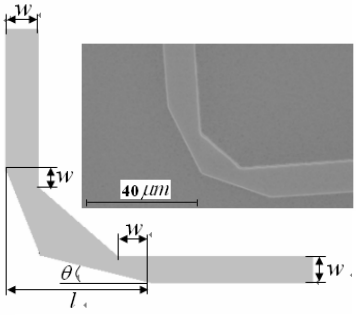

Fig. 5. Schematic picture and SEM morphology of the 90° bend waveguide structure.

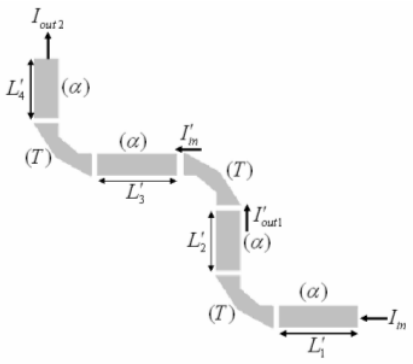

Fig. 6. Schematic picture of the waveguide including three bends.

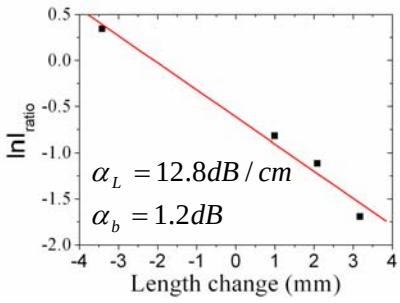

Fig. 7. Plot of $\ln I_{ratio}$ versus the change of waveguide length ΔL for amorphous BST0.7 film waveguide with about 5 μm width and 200 nm thickness.

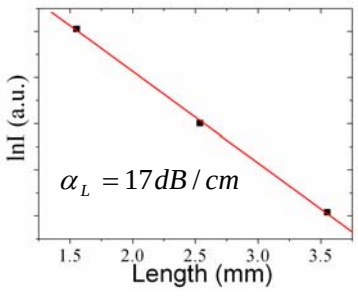

Fig.8. Plot of $\ln I$ versus the waveguide length for poly-crystalline BST0.7 film waveguide with about 5 μm width and 350 nm thickness.

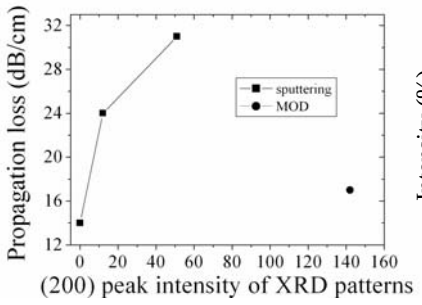

Fig. 9. Plot of optical propagation loss versus (200) peak intensity of XRD patterns.

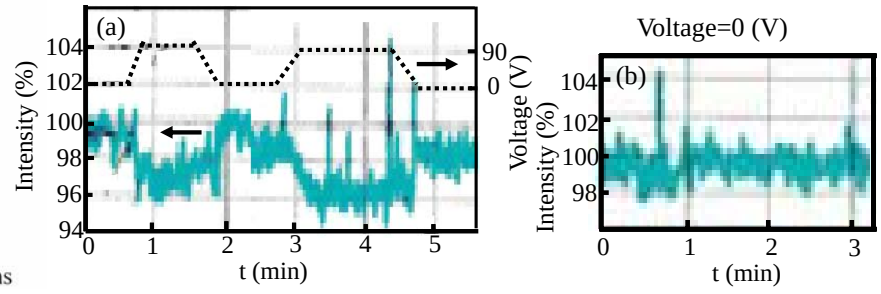

Fig.10. Plot of output light intensity versus time for a Mach-Zehnder switching with 5 μm wide and 350 nm thick poly-BST0.7 core layer when applied bias voltage (a) and no voltage (b).

Groove-Buried Optical Waveguides Based on Metal Organic Solution-Derived $Ba_{0.7}Sr_{0.3}TiO_3$ Thin Films

Zhimou Xu, Yuichiro Tanushi, Masato Suzuki, Keita Wakushima and Shin Yokoyama
Research Center for Nanodevices and Systems, Hiroshima University,
1-4-2 Kagamiyama, Higashi-Hiroshima 739-8527, Japan

Motivation:

- The optical interconnection in LSI is being investigated in order to overcome the signal speed limit induced by the global metal interconnection.
- Our research target is to realize the compact optical switching using electro-optic materials, which can be monolithically integrated in LSI.
- In this work, $Ba_{0.7}Sr_{0.3}TiO_3$ (BST0.7) films are studied for the application to the electro-optic materials of the compact optical switch.

Experiments:

- BST films were formed by spin-coating method. A waveguide and a Mach-Zehnder optical switching were fabricated by traditional micro-fabrication.
- The multilayer films of desired thickness were annealed in open air in a conventional box furnace.
- The phase structure was analyzed by X-ray diffraction (XRD). The morphology was measured by AFM and SEM.

Results and discussion

Layout schematic of optical switching in LSI

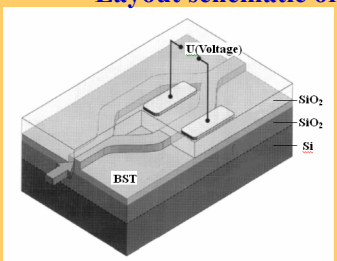

MZI optical switching or modulator

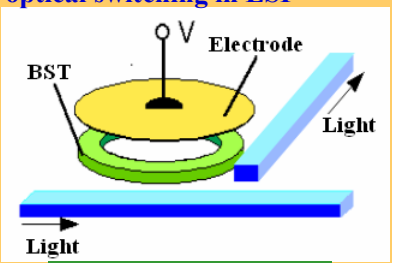

Micro-ring optical switching

Good roughness for BST thin films

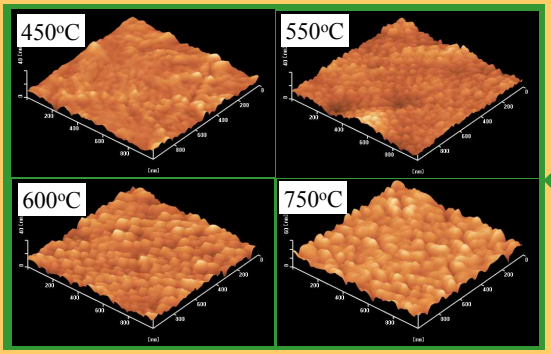

RMS roughness of BST films with 180 nm thickness is smaller than 5 nm.

A complete pseudo-cubic perovskite phase of BST0.7 has already begun to appear at 550℃ for 2h-postannealing. The lower crystallized temperature for BST0.7 film is very helpful to be integrated in optoelectronic integrated circuits (OEICs).

High transparency for BST thin films

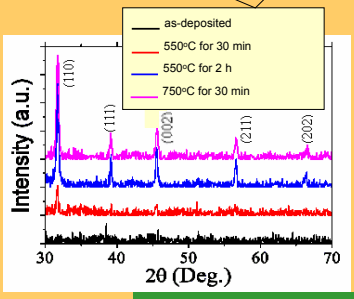

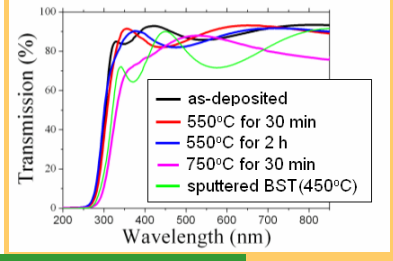

About 220 nm BST film spin-coated on fused quartz

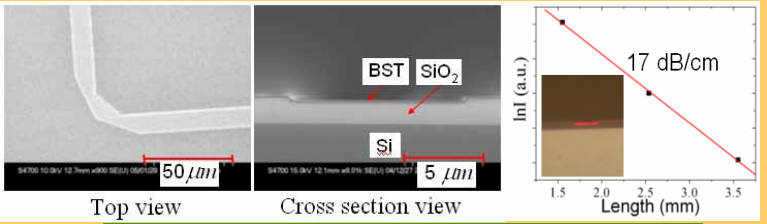

SEM pictures and performance for a poly-BST groove waveguide.

Structure of poly-BST optical switching

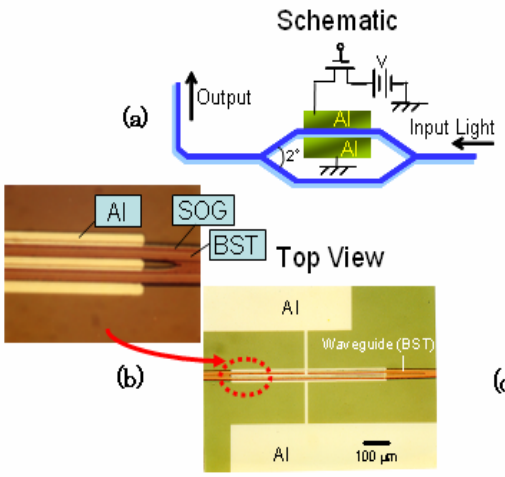

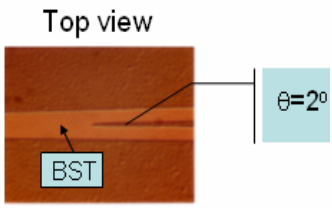

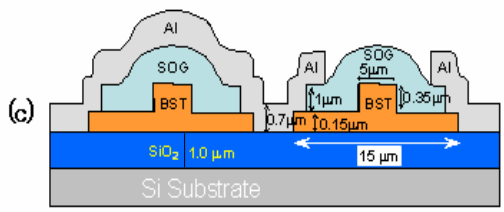

Performance of poly-BST optical switching

λ = 632.8 nm L = 0.6 mm (L : Al electrode length)

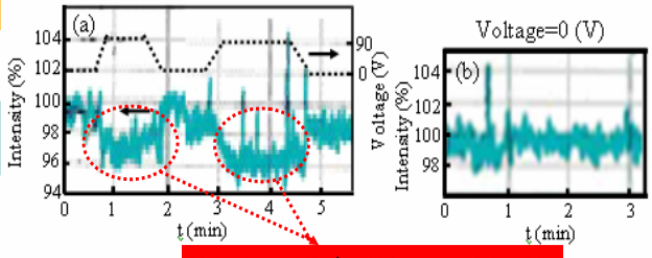

Light phase shift, Δφ=16.2°, $\gamma_{eff(BST)}$=0.4 pm/V

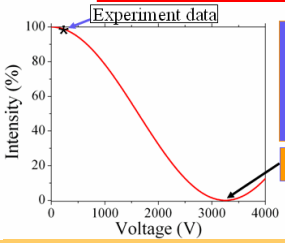

$n_{e(BST)}$=2.3
G=15mm
$\gamma_{eff(BST)}$=0.4pm/V
λ=632.8nm
L=0.6mm

V_{π}=3250V

The optical phase shift of poly-BST MZI optical switching was realized.

Conclusion

① *The crystalline BST0.7 films have been grown directly on SiO_2/Si substrate by novel MOD technique with relatively lower postannealing temperature 550℃. The lower crystallized temperature for BST0.7 film is very helpful to be integrated in OEICs.*

② ***The optical propagation losses of amorphous BST and poly-BST groove waveguides are respectively about 4 dB/cm and 17 dB/cm at the wavelength of 632.8 nm.***

③ ***The optical phase shift of 16.2° was realized for the MZI optical switching with 5μm wide and 350 nm thick poly-BST core layer when the applied dc voltage was 90 V. The efficient electro-optic coefficient is about 0.4 pm/V at the wavelength of 632.8 nm.***